Time Domain Analysis of SAW Reflectors

ROGER D. FILDES AND BILL J. HUNSINGER

Abstract—**A time domain analysis of high-reflectivity SAW reflector arrays is shown to yield values of stripe reflectivity, center frequency, and effective reflection plane penetration. An examination of the approach shows that the results are insensitive to device losses, RF coupling, and transducer response. Experimental results confirm the validity of the technique.**

I. Introduction

REFLECTOR gratings have traditionally been analyzed in terms of their frequency response using a transmission-line model [1]–[3]. Accurate determination of device parameters from a measured frequency response is difficult, however, since device losses, direct transducer response, and RF coupling provide broad-band distortions. Transducer frequency responses, however, are usually transformed to the time domain for analysis. A comparison of theoretical and measured impulse responses aids in the identification, analysis, and improvement of surface wave transducer response.

This paper applies a similar time domain analysis to reflector arrays. Such an approach is shown to give additional insight into device performance and to overcome some of the difficulties in the measurement of device parameters. The determination of center frequency and the normalized reflector stripe impedance z is shown to be simple and essentially independent of reflector losses, RF coupling, and transducer responses. Location of the effective reflection plane L_p for the lossless case may also be determined.

II. Impulse Response Determination

A. Graphical Approach

Initially a lossless array of reflector stripes with uniform reflectivity and gap and stripe widths is assumed. It is seen in Fig. 1(c) that the impulse response $r(t)$ of such an array is a series of pulses separated by 2τ, where τ is the width of a gap or stripe divided by the surface wave velocity [4]. Fig. 1(b) shows that the magnitude of a given pulse is dependent upon the number of propagation paths contributing to that pulse and upon the values of reflection and transmission coefficients of the edges encountered by each such path. The reflection and transmission coefficients for a wave encountering a stripe are defined as $R_i=(z-1)/(z+1)$ and $T_i=2z/(z+1)$, and the coefficients for a wave encountering a gap as $R_0=(1-z)/(1+z)$ and $T_0=2/(1+z)$. An expression for the pulse at any given time may be written as a function of these parameters. In practice, these expressions may be simplified by using only two parameters, R and T, where $R=R_i=-R_0$, and $T=\sqrt{T_iT_0}$.

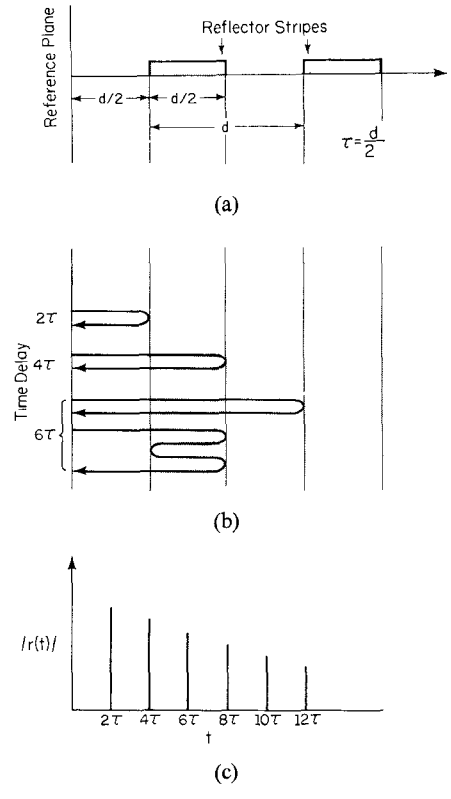

Fig. 1. Graphical impulse response analysis. (a) Uniform reflector array. (b) Array reflection components. (c) Impulse response.

A graphical illustration of the first three pulses from a reflector array is shown in Fig. 1(b). The first pulse occurs at time 2τ and has a magnitude of R, while the second pulse occurs at 4τ and has a magnitude of $-RT^2$. The third pulse at time 6τ is the sum of two components, RT^4 and $-R^3T^2$. In principle, this type of analysis may be extended to longer times and to arrays of arbitrary length and is used in determining the expressions given in Table I. The expressions assume that the number of stripes in the array N is sufficiently large that the impulse response at a given time is equivalent to the semi-infinite array response.

Fig. 2 qualitatively depicts the magnitudes of the first four components of the pulses as a function of time. It is seen that each component builds to a peak and then

Manuscript received June 13, 1977; revised March 29, 1978. This work was supported by the Joint Services Electronics Program (U.S. Army, U.S. Navy, and U.S. Air Force) under Contract DAAB-07-72-C-0259.

The authors are with the Coordinated Science Laboratory, University of Illinois at Urbana-Champaign, Urbana, Illinois 61801.

0018-9480/79/0200-0194$00.75 ©1979 IEEE

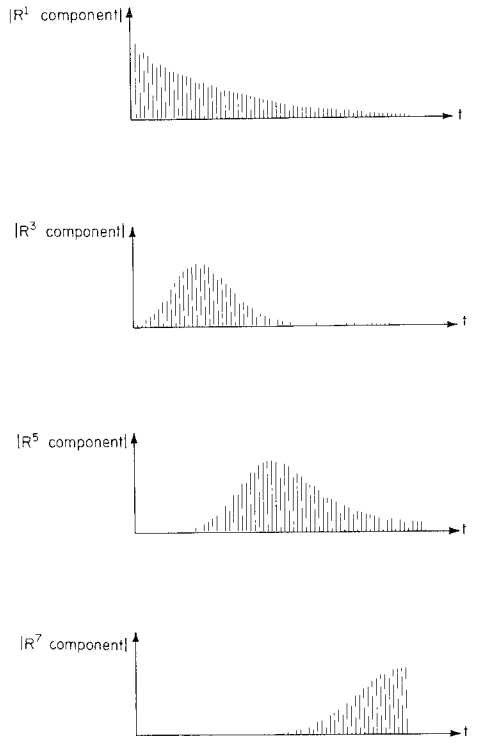

Fig. 2. Qualitative impulse response component magnitudes.

TABLE I

Time Delay	Pulse No (i)	Reflection Components R^1	R^3	R^5	R^7	R^9	R^{11}	R^{13}
2τ	1	$+R$						
4τ	2	$-T^2R$						
6τ	3	$+T^4R$	$-T^2R^3$					
8τ	4	$-T^6R$	$+3T^4R^3$	$-T^2R^5$				
10τ	5	$+T^8R$	$-6T^6R^3$	$+6T^4R^5$	$-T^2R^7$			
12τ	6	$-T^{10}R$	$+10T^8R^3$	$-20T^6R^5$	$+10T^4R^7$	$-T^2R^9$		
14τ	7	$+T^{12}R$	$-15T^{10}R^3$	$+50T^8R^5$	$-50T^6R^7$	$+15T^4R^9$	$-T^2R^{11}$	
16τ	8	$-T^{14}R$	$+21T^{12}R^3$	$-105T^{10}R^5$	$+175T^8R^7$	$-105T^6R^9$	$+21T^4R^{11}$	$-T^2R^{13}$

decays, and that components with higher powers of R peak at later times. Noting that successive components of a pulse change sign, it becomes clear that nulls will exist at the times when the sum of the positive components cancels the sum of the negative components.

Each pulse expression is written as a function strictly of R by substituting $\sqrt{1-R^2}$ for T. The values of R which will produce a null at a given time are found by determining the roots of the appropriate expression. For example, a null occurring at time $t=6\tau$ means that the third pulse from the reflector array has a magnitude of zero (see Fig. 1(c)). The sum of the components of the third pulse expression (see Table I) are set equal to zero, and R is then calculated to be $\pm\sqrt{2}/2$. With smaller, more realistic values of R, nulls would not be expected to occur until later times.

Both the graphical derivation of high-order pulse expressions and the solution for the roots of such expressions become an unmanageable task, even with the aid of a computer. Another procedure for determining the impulse response of an array is readily available, however, and is more general in its scope. Transmission-line models have been used extensively in describing the frequency domain of reflectors and, in contrast to the equation analysis above, are easily adapted to include nonuniformities within the reflector array. For simplicity it is decided to utilize such an established model to obtain the frequency domain data and then to transform the data to the time domain.

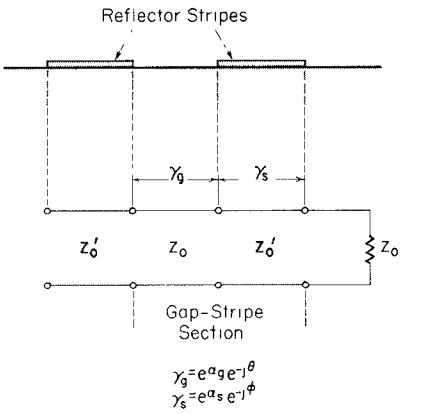

Fig. 3. Transmission-line reflector model.

B. Fourier Transform Approach

The transmission-line model of a reflector array is illustrated in Fig. 3.[1] Reflector stripes are considered to have phase length ϕ, attenuation α_s, and characteristic impedance Z_0', while free surface gaps are represented by phase length θ, attenuation α_g, and characteristic impedance Z_0. The transmission matrix (T-matrix) of the array is calculated by cascading the T-matrices of each successive gap-stripe section and is then converted to a scattering matrix. The reflection coefficient S_{11} represents the reflectivity of the array so that the frequency response $\Gamma(\omega)$ is found by plotting S_{11} versus frequency. The impulse response of the reflector array is obtained by Fourier transforming $\Gamma(\omega)$.

The theoretical frequency response of a lossless 800 stripe array with $\lambda/4$ stripes and gaps and normalized impedance $z=Z_0'/Z_0=0.992\,24$ is shown in Fig. 4(a). It is quite similar to responses presented by Lakin, Haydl, and Suzuki [2], [5], [6]. The envelope of the theoretical impulse response of the reflector, obtained by transforming $\Gamma(\omega)$, is pictured in Fig. 4(b). For the theoretical frequency of 98.38 MHz, the primary reflections are time limited to a little over 8 μs. The long time duration of the repetitive lobes, therefore, indicates that multiple reflections within the array are indeed a significant phenomenon.

Near the center frequency of a high-reflectivity array, little energy reaches the end of the array so that its response closely approximates that of an infinite array. Significant energy of off-frequency signals penetrates to

[1]Second-order mechanisms such as stored energy are not considered.

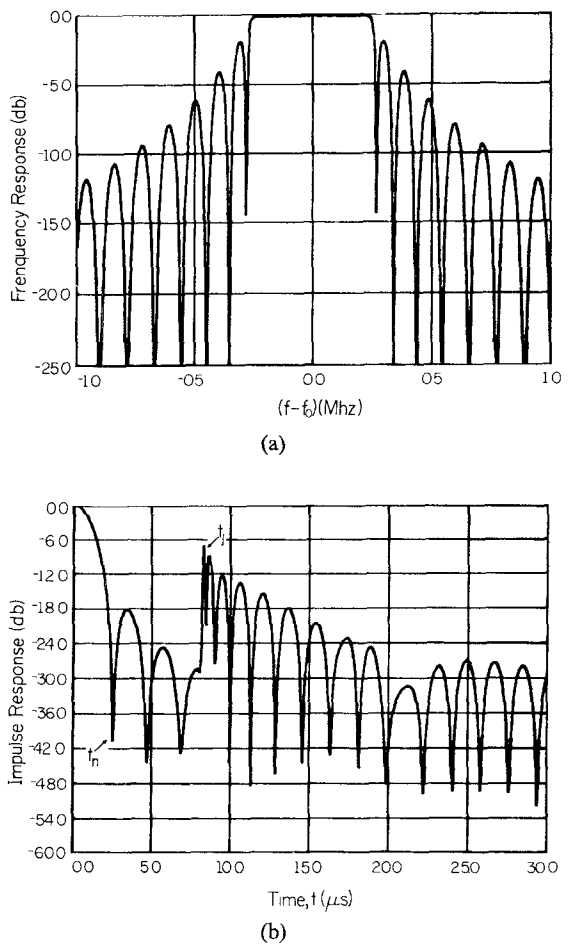

Fig. 4. Theoretical reflector array responses. (a) Frequency response. (b) Impulse response.

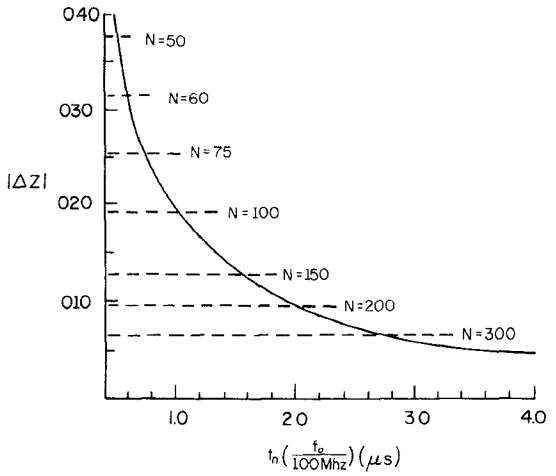

Fig. 5. Characteristic impedance mismatch versus first null time.

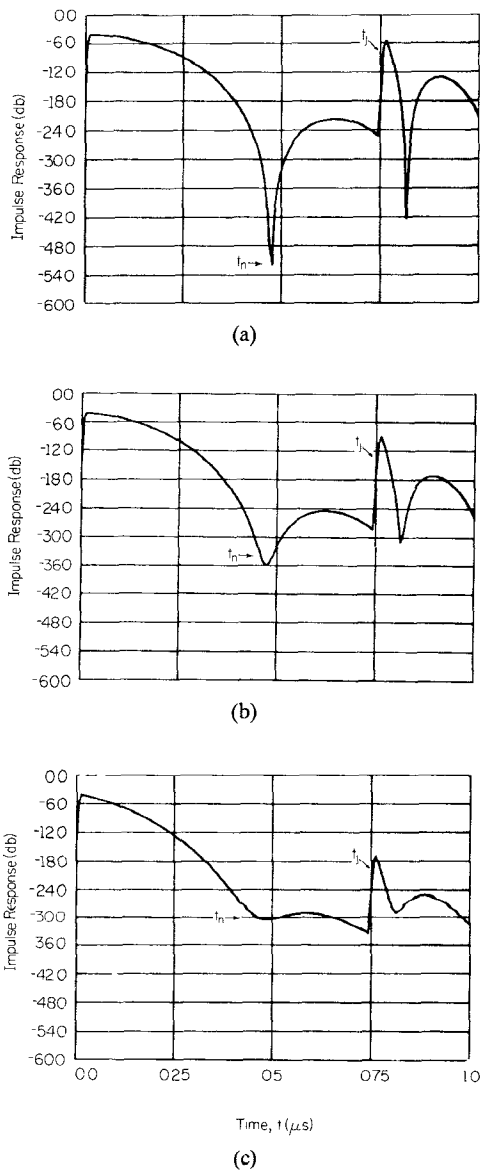

Fig. 6. Effects of stripe loss: $z=0.960$, $f_0=100$ MHz, $N=75$. (a) $\alpha_g=0$, $\alpha_s=0$, $|\Gamma(\omega_0)|=0.9956$. (b) $\alpha_g=0$, $\alpha_s=0.0027$ Np/stripe, $|\Gamma(\omega_0)|=0.9419$. (c) $\alpha_g=0$, $\alpha_s=0.009$ Np/stripe, $|\Gamma(\omega_0)|=0.8362$.

the end of a typical reflector, however, causing its response to such signals to be affected. The lack of multiple reflections at the end of the array causes it to act as a highly localized discontinuity. This effect results in the occurrence of a sudden jump in an array's reflectivity impulse response as seen in Fig. 4(b) at time t_j. The center frequency of the array may thus be calculated from the equation $f_0 = N/t_j$, where N is the total number of reflector stripes.

The multiple reflections within the array interact to produce a series of impulse response nulls as predicted in the graphical analysis section. For a given center frequency, the location of the first null t_n has a one-to-one correspondence to $|R|$. For small values of reflectivity, $\Delta z = (1-z)$ is approximately equal to $2R$, so that $|\Delta z|$ may be considered as a function of t_n and f_0. This relationship is plotted in Fig. 5. The type of substrate and reflector stripes used determine the sign of Δz, so that z may be determined from the graph by locating the appropriate $(t_n f_0/100\text{-MHz})$ ratio on the x axis. This relationship is independent of N, as long as N is large enough that the first null occurs before time t_n. This is true for high-reflectivity reflector arrays where $\Gamma(\omega_0) = (z^{2N}-1)/(z^{2N}+1) \geqslant 0.957$. The dashed lines represent the lower limit of $|\Delta z|$

which may be read from the graph for a given N, ensuring that $t_n < t_j$. Also, once z is determined, the location of the effective reflection plane may be calculated as $L_P = 1/4|\Delta z|$ wavelengths into the array, assuming there are no propagation losses [7].

Uniform attenuation ($\alpha_g = \alpha_s$) in an array decreases the magnitude of each pulse component at a given time by an identical amount, so output nulls remain unaffected. Assuming reasonably small changes in the attenuation factor between successive output pulses, output maxima will also remain the same. Thus the location of t_n and t_j are not affected by uniform loss. Fig. 6 shows the effect of nonuniform attenuation ($\alpha_g \neq \alpha_s$), illustrating that such loss has negligible effect on the position of t_j or the minimum t_n for any loss factor acceptable in a resonator reflector. The curve of Fig. 5 is thus independent of such losses so that the determination of z is valid in spite of the presence of array attenuation. With an accurate knowledge of z, the theoretical array reflectivity at center frequency, $\Gamma(\omega_0) = (z^{2N} - 1)/(z^{2N} + 1)$ may be calculated and compared to measured reflectivity for a determination of attenuation losses.

Another approach to the determination of z without the use of a graph is given in the Appendix.

III. Experimental Results

A test device constructed to verify the principles of practicality of the above approach of analysis is shown schematically in Fig. 7. The reflector array consists of 800 shorted Al stripes on ST-Quartz, and both transducers and reflector stripes are ~4000-Å thick. The transducers are designed with $\lambda/8$ fingers to minimize the effect of reflections from their edges. The measured frequency response is pictured in Fig. 8(a). The reflector response is masked by RF coupling, introducing uncertainty into the analysis of the original frequency data. The impulse response envelope obtained by Fourier transforming the frequency data is shown in Fig. 8(b). The time domain plot looks much like expected, noting that the effect of RF coupling is separated from the reflector response, in contrast to the original frequency data. Direct transducer response on this device was suppressed with the use of a unidirectional transducer as the output transducer [8]. If a unidirectional output transducer is not used, the direct transducer response is localized in the time domain and does not affect t_n or t_j. The output transducer should, however, be located far enough from the array so that the direct transducer response does not appreciably affect the apparent value of t_s, which is taken as the zero time reference. Since $N = 800$ and $z < 1$ (Al fingers on quartz), the center frequency is calculated to be 98.52 MHz and $z = 0.9922$, indicating that the previous theoretical model with parameters $f_0 = 98.38$ MHz and $z = 0.992\ 24$ should give a close fit of measured data. Fig. 8(c) shows the superposition of the theoretical and measured impulse responses.

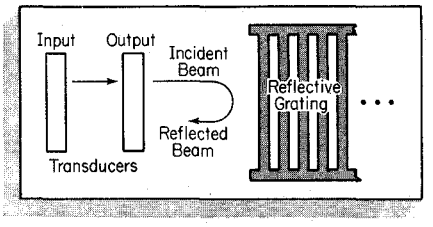

Fig. 7. Test device schematic.

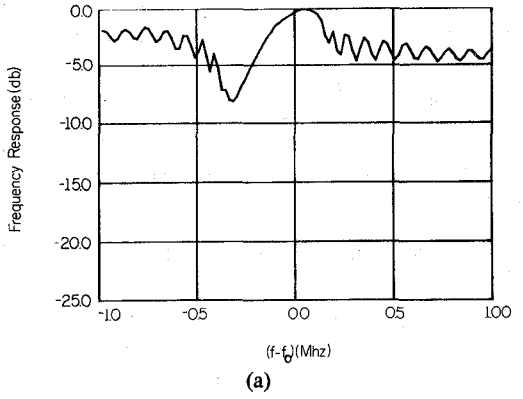

(a)

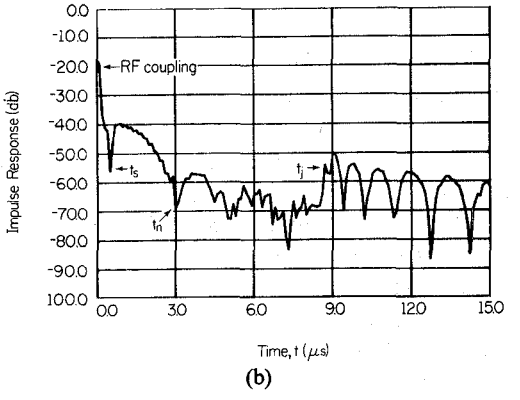

(b)

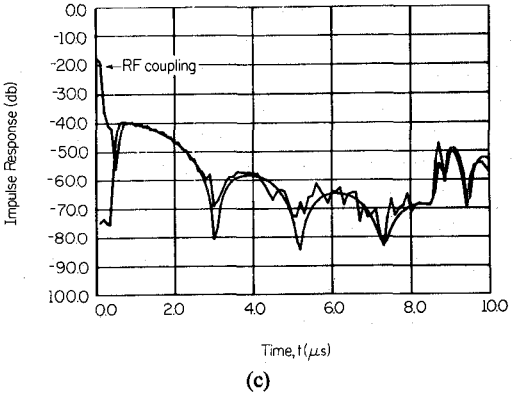

(c)

Fig. 8. Experimental test device responses. (a) Measured frequency response. (b) Experimental impulse response. (c) Superposition of experimental and theoretical impulse responses.

IV. Summary

An approach to the time domain analysis of high-reflectivity uniform SAW reflector arrays has been presented. Accurate determination of center frequency and normal-

ized reflector stripe impedance has been shown to be straightforward and insensitive to losses, RF coupling, and transducer coupling.

The procedure for calculating these parameters is as follows:

1) measure the frequency response of the device $\Gamma(\omega)$;
2) transform $\Gamma(\omega)$ to obtain the impulse response $r(t)$;
3) note the values of t_n and t_j (as referred to t_s);
4) center frequency is equal to N/t_j;
5) $\Delta z = (z-1)$ may be read from graph in Fig. 5, or z may be approximated from the equation

$$\underset{<1}{z>1} \approx \exp\left[\frac{t_j \ln(3\pm 2\sqrt{2})}{(0.918)Nt_n}\right] \quad \text{(see Appendix)}$$

6) for $\alpha_s = \alpha_g \approx 0$, effective reflection plane penetration is given by $L_P = 1/4|z-1|$ wavelengths.

Initial results also indicate that the analysis is readily extendable to withdrawal weighted reflector arrays. Future work may produce similar procedures for determination of other parameters such as stored energy and device losses.

V. Appendix

While a tabulated graph such as that in Fig. 5 is quite easy to use, z may be closely approximated by a direct calculation when a graph is not available. Returning to the equation analysis of Section II, it is recalled that $|R| = \sqrt{2}/2$ is the solution for the case of a null occurring at $t = 6\tau$. Of this total time of 6τ, 2τ is simply the net delay time between the reference plane and the front edge of the reflector array. The actual time duration of reflections within the array which are involved in producing the null is thus 4τ. Since $|R| = \sqrt{2}/2$, each edge reflects one-half of any incident power so that τ is the separation time of successive "half-power reflectors." The 4τ interaction time of the array is noted to be four times this separation time. If this observation is extendable to arrays with smaller values of $|R|$, the first anticipated null of an array would be at $t = (4t_h + 2\tau)$, where t_h is the time length of a section of stripes with a net reflection magnitude of 0.707 or one-half power.

For $z = 0.992$ 24, 113 reflector stripes have a net reflectivity of -0.707 or one-half power. With $\tau = 1/4f_0 = 2.54$ ns, the corresponding time separation between successive half-power reflector sections is then 0.574 μs. By the above correlation the expected time of the first null is then $4(0.574) + 2(0.0025) = 2.30$ μs. In Fig. 4 the calculated null t_n is seen to be ~ 2.45 μs which is close but not exactly equal to the anticipated value. That some extra time is required is to be expected. Examination of the earlier example for $R = \pm 0.707$ (discrete half-power reflectors) shows that interactions between three edges was required to produce the null. In the distributed case an impulse signal needs to penetrate slightly into the third half-power section before interactions in the array correspond to the interactions between three half-power edges. This extra time will be constant for a given t_n, however, so that the calculated or measured t_n need only be corrected by a determinable factor γ in order to use the simple concept as proposed.

$N_0 = \gamma t_n N/2t_j$ is the number of reflectors which have a net reflection magnitude of $\sqrt{2}/2$, so that z may be calculated from the equation

$$\underset{<1}{z>1} \approx \exp\left[\frac{\ln(3\pm 2\sqrt{2})}{2N_0}\right].$$

It has been empirically determined that it is sufficient to remember a value of about 0.918 for γ in most practical experimental work, resulting in the equation

$$\underset{<1}{z>1} \approx \exp\left[\frac{t_j \ln(3\pm 2\sqrt{2})}{(0.918)Nt_n}\right].$$

References

[1] E. K. Sittig and G. A. Coquin, "Filters and dispersive delay lines using repetitively mismatched ultrasonic transmission times," *IEEE Trans. Sonics Ultrason.*, vol. SU-15, pp. 111–119, 1968.
[2] K. M. Lakin and T. R. Joseph, "Surface wave resonators," in *1975 Ultrason. Symp. Proc.*, Cat. no. 75 CHO 994-4SU, pp. 269–279.
[3] W. R. Shreve, "Surface wave resonators and their use in narrow-band filters," in *1976 Ultrason. Symp. Proc.*, Cat. no. 76 CH 1120-5SU, pp. 706–713.
[4] Herbert Matthews, *Surface Wave Filters*. New York: Wiley Interscience, 1977, chap. 9.
[5] W. H. Haydl *et al.*, "Multimode SAW resonators—A method to study the optimum resonator design," in *1976 Ultrason. Symp. Proc.*, Cat. no. 76 CH 1120-5SU, pp. 287–296.
[6] Y. Suzuki *et al.*, "Some studies on SAW resonators and multiple-mode filters," in *1976 Ultrason. Symp. Proc.*, Cat. no. 76 CH 1120-5SU, pp. 297–302.
[7] P. Cross, "Reflective arrays for SAW resonators," in *1975 Ultrason. Symp. Proc.*, Cat. no. 75 CHO 994-4SU, pp. 241–244.
[8] R. D. Fildes and B. J. Hunsinger, "Application of unidirectional transducers to resonator cavities," in *1976 Ultrason. Symp. Proc.*, Cat. no. 76 CH 1120-5SU, pp. 303–305.